Published in final edited form as:
Circ Res. 2013 March 1; 112(5): 863–874. doi:10.1161/CIRCRESAHA.112.279315.

Noninvasive Electrocardiographic Imaging (ECGI) of Arrhythmogenic Substrates in Humans

Yoram Rudy
Cardiac Bioelectricity and Arrhythmia Center (CBAC), Washington University in St. Louis, St. Louis, MO 63130

Abstract

Cardiac excitation is determined by interactions between the source of electrical activation (membrane depolarization) and the load that cardiac tissue presents. This relationship is altered in pathology by remodeling processes that often create a substrate favoring the development of cardiac arrhythmias. Most studies of arrhythmia mechanisms and arrhythmogenic substrates have been conducted in animal models, which may differ in important ways from the human pathologies they are designed to represent.

Electrocardiographic imaging (ECGI) is a noninvasive method for mapping the electrical activity of the heart in humans, under "real world" conditions. This review summarizes results from ECGI studies of arrhythmogenic substrates associated with human clinical arrhythmias. Examples include: heart failure, myocardial infarction scar, atrial fibrillation and abnormal ventricular repolarization.

Keywords

Cardiac arrhythmia; Electrophysiology; Myocardial infarction; Heart failure; Atrial fibrillation

Introduction

The process of cardiac excitation involves generation of the action potential by ionic membrane currents and propagation of the action potential through the multicellular structure of cardiac tissue[1]. The properties of excitation and the development of cardiac arrhythmia are determined by the interaction between the source of electrical activation (membrane depolarization) and the electric load ("sink") that the tissue presents. In the normal heart, the source and sink are properly matched and excitation is robust. With pathology, electrophysiological and structural changes ("remodeling") can occur that alter the source – sink relationship, creating a mismatch between source and load that promotes arrhythmic behavior. Pathological changes can affect the membrane excitability (e.g., via

Correspondence: Yoram Rudy, Director CBAC, 290 Whitaker Hall, Campus Box 1097, One Brookings Drive, St. Louis, MO 63130-4899, Phone: 314.935.8160; Fax: 314.935.8168; rudy@wustl.edu, URL:http://rudylab.wustl.edu.

Subject Codes:
5, 11, 106, 124, 171

Disclosures: Yoram Rudy co-chairs the scientific advisory board and holds equity in CardioInsight Technologies (CIT). CIT does not support any research conducted by Y.R., including that presented here.

downregulation of the fast sodium current), modify the tissue structure (e.g., by affecting gap-junctions expression and distribution, and by causing fibrosis), or both. In many cases, the remodeling process is dynamic and progressive, creating an arrhythmogenic substrate that changes with time.

Most studies of arrhythmia mechanisms and arrhythmogenic substrates have been conducted in animal models. While providing invaluable information, extrapolation of results to the human heart is not obvious because of major species differences and model limitations in representing human disease processes. Species differences exist at multiple scales of the cardiac system, from the ion-channel profile of individual cells, to whole heart organization (e.g., spatial heterogeneity of ion-channel expression and of calcium cycling, Purkinje system architecture). Human disease processes can only be approximated by animal models. For example, arrhythmias and substrate associated with myocardial infarction (MI) have been studied extensively in a canine model where the MI substrate was produced by 5-day ligation of the left anterior descending coronary artery[2, 3]. This model substrate, while representing important aspects of post-MI remodeling, is likely to differ from an infarct in the elderly patient with 20 years history of coronary heart disease.

Electrophysiologic studies in the human heart under “real world” conditions have been hampered by the unavailability of noninvasive imaging methods (similar to CT or MRI) for high resolution mapping of cardiac electrophysiology and arrhythmia. We recently developed Electrocardiographic Imaging, ECGI (also called Electrocardiographic Mapping, ECM) as a noninvasive modality for human application (both research and clinical)[4, 5], and used it to study arrhythmogenic substrates and arrhythmias in patients. ECGI reconstructs potentials, electrograms, activation sequences (isochrones) and repolarization patterns on the heart surface. The reconstruction is performed simultaneously over the entire heart and is done continuously on a beat-by-beat basis.

In this review, insights from ECGI studies of human electrophysiologic substrates associated with clinical arrhythmias are summarized. The article focuses on ECGI substrate imaging, not on details of the ECGI method, its clinical application, or the basic mechanisms of cardiac arrhythmias. Following a brief description of the ECGI methodology, the representative examples listed below are provided:

1. The Electrophysiologic (EP) substrate in heart failure;
2. The EP ventricular substrate after MI and arrhythmia associated with the post-MI scar;
3. Progressive remodeling in atrial fibrillation (AF);
4. The EP substrate associated with abnormal action potential repolarization.

The ECGI Method

The electric potential field ϕ, generated by excitation of the heart in the surrounding torso volume between the epicardium and the body surface, obeys Laplace’s equation[6]:

$$\nabla^2\phi=0 \quad [1]$$

where $\phi = \phi_T$ on the torso surface and $\phi = \phi_E$ on the epicardium;. ∇^2 is the Laplacian operator. ϕ_T can be measured noninvasively by electrodes placed on the body surface. The objective of ECGI is to compute ϕ_E from the measured ϕ_T. Application of Green’s second theorem and discretization of the epicardial and torso surfaces into triangular elements provides the following matrix equation relating ϕ_T to ϕ_E[6, 7]:

$$\phi_T = A\phi_E \quad [2]$$

where ϕ_T is a vector of (measured) torso potentials and ϕ_E is a vector of (unknown) epicardial potentials. The matrix A contains the geometric information that relates the two (heart and torso) surfaces. Equation [2] computes ϕ_T from given ϕ_E, a formulation that defines the forward problem of electrocardiography. ECGI requires to invert this problem and compute ϕ_E from a known ϕ_T, a procedure that constitutes the inverse problem of electrocardiography. The inverse problem is ill-posed[8, 9], meaning that even small errors in the measured ϕ_T data (measurement noise, electrodes positions) can result in very large (unbounded) errors in the computed ϕ_E. To suppress such errors, we have applied two different computational schemes in the ECGI application: Tikhonov regularization[8, 9] (a method that imposes constraints on ϕ_E) and the generalized minimal residual (GMRes) iterative technique[10, 11].

The ECGI algorithm requires two sets of data: the electrocardiographic potential over the entire torso surface (ϕ_T) and the geometries of the heart and torso surfaces (matrix A)[12]. To obtain ϕ_T, 250 electrodes mounted on strips are applied to the patient's torso (both anterior and posterior) and connected to a portable mapping system (Figure 1). Each electrode contains a marker that is visible in a computed tomography (CT) scan. The patient undergoes thoracic noncontrast gated CT with axial resolution of 3mm, providing the epicardial geometry and torso electrode positions in the same image. The torso surface potentials, recorded by the 250 electrodes, are sampled at 1-ms intervals. The recorded torso potential and CT-derived geometrical information provide the input data for the ECGI algorithm, which constructs noninvasively epicardial potentials, electrograms, activation sequences (isochrone maps) and repolarization patterns. The reconstruction is performed during a single beat and does not require accumulating data from many beats. This property makes it possible to image non-sustained and polymorphic arrhythmias, and arrhythmias that are not hemodynamically tolerated.

At present, CT is the method of choice for obtaining noninvasively the individual heart-torso geometrical relationship in a given patient. We use non-contrast CT at very low radiation (less than 2 rads), and this has been decreasing with advances in CT technology. We only obtain one CT scan at the first ECGI study. In follow-up studies we reapply the body surface electrode strips at the same positions as in the first study (using anatomical and external markers), eliminating the need for a repeat CT. In principle, other anatomical imaging methods can be used to obtain the geometry. MRI could be used once it has been made safe to apply in patients with implanted devices (a large segment of the cardiac patients population). Ultrasound could probably also replace CT, once high quality 3-dimensional echocardiography becomes available.

ECGI has been validated extensively under different physiological and pathological conditions in animal models and human studies (see examples[13-18]). In particular, the torso-tank experimental setup[13] provided well-controlled experimental conditions that mimicked the clinical situation. This preparation consisted of a tank in the shape of a 10-year-old boy's torso filled with an electrolytic solution, with a perfused dog heart suspended within the torso volume in the correct anatomical position. The system included 384 torso surface electrodes and 384 rods with electrodes at their tips. The rods were pushed towards the heart so that their tips created an epicardial envelope. Potentials measured by the torso surface electrodes were used as input data to compute noninvasively epicardial potentials. These were then compared to the "gold standard" of directly measured epicardial potentials by the rod-tip electrodes. Validation protocols were conducted in normal and infarcted canine hearts during sinus rhythm, multiple-site pacing, and reentrant ventricular tachycardia.

Correlation coefficients between noninvasively reconstructed and directly measured epicardial electrograms were > 0.9 for 72% of all epicardial locations, indicating very good agreement. In infarcted hearts, ECGI reconstructed accurately low potentials and low amplitude fractionated electrograms within the infarct scar region. ECGI was also shown to reconstruct repolarization properties accurately and to localize areas of increased dispersion of repolarization (induced by myocardial warming and cooling) noninvasively[18]. Validation in humans included comparison to direct intra-operative mapping in open heart surgery patients during sinus rhythm and RV epicardial and endocardial pacing[17]. Unlike the tank-torso experiments, ECGI and direct epicardial mapping could not be performed simultaneously and under identical conditions in the intra-operative study. Despite this limitation, it was shown that ECGI reconstructed isochrones captured the sites of earliest activation, areas of slow conduction, and the general excitation pattern. Through comparison with simultaneous invasive catheter mapping and localization of pacing electrodes by CT, it was determined that the spatial accuracy for determining initiation sites (induced by pacing) noninvasively with ECGI was about 6 mm.

The ECGI method for computing epicardial potentials from body surface potentials relies on the assumption that Laplace's equation [1] holds in the torso volume conductor between these two bounding surfaces (the torso surface and the epicardium). This reflects the fact that there are no active electrical sources (no excitable cardiac tissue) in this volume. Extension of the approach to the endocardium violates this assumption because during cardiac excitation there are active sources within the myocardium. Therefore, reconstruction of endocardial excitation requires additional assumptions (that may bias the solution in a non-physiological way) or the application of alternative approaches. One alternative approach is the model-based method (using a bi-domain model of the heart) that computes only local activation times (isochrones) but not the entire electrograms[19,20]. This approach was used successfully to image pre-excitation in Wolff-Parkinson-White patients[19] and to reconstruct activation sequences in congestive heart failure patients undergoing cardiac resynchronization therapy[20].

All protocols were approved by the Washington University Human Research Protection Office, and informed consent was obtained from all patients.

EP Substrate and Cardiac Resynchronization Therapy (CRT) in Heart Failure

Heart failure (HF) is a progressive disease that is highly prevalent and associated with high mortality[21]. Up to 50% of deaths in HF patients are sudden, and a majority of the deaths are from ventricular tachyarrhythmias[22]. On the other hand, arrhythmias can contribute to the HF by causing cardiomyopathy through remodeling processes[23,24]. In HF, abnormal cellular electrophysiologic processes and calcium cycling are superimposed on structurally remodeled tissue, resulting in compromised AP propagation (slow conduction, conduction block)[25-27]. Through abnormal calcium cycling and AP repolarization, HF also promotes arrhythmia triggers in the form of delayed and early afterdepolarizations[28]. Much is known (and is being intensely researched) regarding the molecular basis for the cellular electrophysiologic and calcium cycling (contractile) changes in HF. At the level of the whole-heart, human data for mechanical contraction are available from tagged MRI and echocardiographic noninvasive imaging studies[29,30]. Body-surface electrocardiographic characteristics in many HF patients include a wide QRS complex and left bundle branch block (LBBB) pattern, indicative of delayed and dyssynchronous activation, predominantly of the left ventricle (LV)[31]. However, detailed understanding of the spatio-temporal excitation pattern in the failing human heart has been lacking. We have used ECGI, taking

advantage of its noninvasive nature, to fill some of this gap and provide insight into the substrate-related ventricular activation patterns in heart failure patients[32].

Figure 2 shows ECGI epicardial activation (isochrones) maps of native (non-paced) rhythm from four HF patients[32]. In all cases, right ventricular (RV) epicardial activation started from a breakthrough site (circular isochrones), in a location consistent with activation of the normal, non-failing human heart[5]. This property indicates normal RV activation via the right bundle of the specialized conduction system. From the breakthrough site, activation spreads radially and uniformly in the RV, with latest activation occurring at the basal or anterior/inferior paraseptal regions, as in normal hearts. Mean duration of RV activation (eight patients) was 25ms.

In contrast to RV activation, LV activation was abnormal and delayed in all patients, accounting for the LBBB pattern of the body surface ECG. Importantly, and different from RV, details of the LV activation patterns were heterogeneous and differed between patients, with variability in the location of the latest activation (blue). In patient 7 (Panel A) LV conduction was from apex to lateral base; inferior to anterolateral conduction was the pattern in patient 5 (B); combined activation from apical, inferior and superior LV was mapped in patient 1 (C); in patient 3 conduction was anterior to inferoposterior. In the patients of Figure 2, anterior line(s)/region(s) of block (black; defined by > 50 ms activation delay across) prevented the activation from spreading further into the LV after crossing the septum from the RV; it spread in a U-shaped pattern to reach the lateral wall by way of the apical or inferior LV (as observed by endocardial catheter mapping also)[33]. Interestingly, during subsequent pacing protocols some of the block regions shifted, indicating their functional nature, while others remained unchanged, suggesting the presence of an anatomical obstacle. Consistent results but with less inter-patient variability were obtained by Berger et al.[20] using the activation time reconstruction approach. In their study, congestive heart failure patients showed right-to-left septal activation with the latest activation epicardially in the lateral wall of the left ventricle. Biventricular pacing resulted in resynchronization of the ventricular activation sequence and decrease of total LV activation duration compared to intrinsic conduction.

Cardiac resynchronization therapy employs biventricular pacing to restore ventricular synchrony; it attempts to advance in time electrical activation of the greatly delayed region of late LV activation. CRT improves patients' symptoms, LV performance and long term survival[34]. For reasons that are not clear, approximately 33% of patients do not respond to CRT. Short term improvement is likely due to more efficient pumping action of the synchronized LV. Long term improvement involves reverse-remodeling of molecular components and processes[35]. The ability to image the electrophysiologic substrate with ECGI and the inter-patient heterogeneity of the substrate have implications to CRT. The degree of resynchronization that is achieved with CRT depends on the site of LV lead placement. Based on the ECGI-imaged sequence of native activation (Figure 2), the region of most delayed LV activation could be determined in a patient-specific manner for placing the pacing lead to maximize synchrony. In addition, information on the electrophysiologic properties of the substrate in a given patient's heart could also be considered. For example, lead placement in areas of unexcitable tissue and regions of conduction block or slow conduction could be avoided. We conducted an ECGI study inpediatric heart failure patients with congenital heart disease undergoing evaluation for CRT[36]. The study demonstrated that ECGI could be used to evaluate ventricular electrical dyssynchrony and identify suitable candidates for CRT. In addition, ECGI was able to guide resynchronization lead placement to the area of latest electrical activation[36]. The potential role of ECGI in CRT should be evaluated in a large prospective study in the adult population of heart failure patients.

Finally, the observation that RV activation utilized the specialized conduction system suggested that in some cases, bi-ventricular pacing can be replaced by LV pacing alone for CRT. We demonstrated that with optimal atrial-ventricular delay, in three of four patients with AV conduction synchronization was achieved by fusion between intrinsic excitation from the RV and paced excitation from the LV placed electrode (figure 7 in reference 32). The possibility of LV pacing alone for CRT has been studied in patients[37,38,39]. A recent trial evaluated an adaptive pacing algorithm for CRT, demonstrating similar benefit with 44% reduction in RV pacing (LV pacing alone regime) compared to bi-ventricular pacing[40].

The Electrophysiologic Substrate after Myocardial Infarction

Myocardial Infarction (MI) triggers a progressive remodeling process that is associated with high incidence of ventricular arrhythmias in survivors in the days and weeks that follow the initial ischemic event. The time progression of electrical changes has been divided into the acute ischemia phase (first 10-15 minutes after ischemia onset), the sub acute phase (hours after onset), and the healing and healed infarct (days to years after the original ischemic event, once infarct has formed)[41]. Many studies of electrophysiologic and structural properties of the healing and healed MI have been conducted in a canine model in which a transmural infarct was created following 3-5 days ligation of the left anterior descending (LAD) coronary artery[2, 3]. Typically, the infarct substrate is a heterogeneous scar that contains “islands” of surviving excitable myocardium (the “border zone,” BZ), characterized by abnormal cellular electrophysiology and altered structural properties due to remodeling processes[42,43]. These changes result in regions of conduction block, long conduction delays, and slow nonuniform and discontinuous conduction through the infarct substrate[44,45]. These properties are reflected in local electrograms that are fractionated, of small magnitude and prolonged duration[46-48]. In addition, some of the electrograms contain late deflections (“late potentials”) at the end and after the QRS complex[49]. These deflections are thought to reflect late activation within the scar BZ, via slow conduction along surviving fibers.

Presence of block regions and pathways for slow discontinuous conduction promote reentrant arrhythmias. These properties, that can be recognized and localized by their reflection in the local electrograms (low potentials, long duration, fragmentation, late potentials), have been the basis for substrate-based ablation strategies in the treatment of scar-related ventricular arrhythmias[50].

ECGI was performed during sinus rhythm in 24 patients with post-MI scars[51]. The objective was to image the electrophysiologic substrate properties in patients, as reflected in the epicardial potentials and electrograms, and to construct “electrical scar” maps based on the noninvasively reconstructed epicardial electrograms’ characteristics. The electrical scar was identified based on electrogram magnitude (low voltage regions were defined by epicardial electrograms with amplitudes <30% of the maximum in a given patient) and degree of fractionation (number of deflections). Grouping the electrograms that demonstrated both properties (low voltage and fractionation) defined the electrical scar. Figures 3A-3C show a representative example of an electrical scar and electrogram characteristics in the scar region. Figure 3B depicts selected electrograms from the scar region (red) and from regions outside the scar (blue). Scar electrograms are of very low magnitude, as emphasized when plotted on the same voltage scale together with non-scar electrograms in the bottom row of panel B. They are also characterized by fragmentation (fractionation), clearly observed on the expanded scale of panel C. Based on the electrograms, the scar maps in panel A were constructed (red). Two images are shown: the top map was based on the low-voltage criterion alone; the bottom map added the criterion of electrogram fractionation, which eliminated the basal part of the “scar.” Delayed contrast MRI has been used to image anatomical scars. Panel D compares the ECGI-reconstructed electrical scar (red; based on

the low voltage criterion) to the MRI-imaged anatomical scar (yellow). There is good agreement between the two images. The basal portion of the electrical scar that was removed by the fractionation criterion is included in the MRI image. It is possible that this portion reflects epicardial fat, rather than true scar substrate (epicardial fat attenuates electrogram voltages but does not cause fractionation; it also appears as a bright region, suggesting scar tissue, in delayed contrast MRI). Inclusion of the fractionation criterion (not detectable by MRI, which does not image electrical properties) removes this portion of the substrate from the electrical scar image (bottom of Panel A).

Late potentials, reflecting delayed activation during sinus rhythm, were present in subsets of electrograms from within the electrical scar. Examples are shown in Figure 4 (late potentials are highlighted by boxes).

The presence of scar altered the pattern of epicardial activation during sinus rhythm (Figure 3 in reference 51; compared to normal activation in absence of scar [5, 12]). Asymmetrical electrical loading of a propagating wave front at scar borders created lines of conduction block. Scar-related slow conduction regions were also mapped by ECGI. The combination of asymmetrical (unidirectional) block and slow conduction provides conditions for formation of reentry circuits and re-entrant arrhythmias.

Scar-Related Ventricular Tachycardia (VT)

ECGI can image the electrical activation sequence over the entire ventricular surfaces in a single beat. This ability to map noninvasively and continuously the dynamic pattern of excitation during an arrhythmia facilitates the study of clinical VT characteristics in the human heart. A study in twenty- five patients[52] undergoing catheter ablation for a broad range of VT provided information on VT initiation and continuation, and in the context of this review article, on the relationship of VT to the ventricular substrate (anatomical scars and myocardium with abnormal electrophysiological properties). Five patients had reentrant VT, with reentry activation patterns related to regions of myocardial scar. An example is shown in Figure 5. Single-photon emission computed tomography (SPECT) images identified an area of scar from a previous MI in the inferior septum (dark blue in Figure 5C). ECGI activation map during VT is shown in panel B; activation movie is provided as Online Movie I. Earliest activation is in the inferior basal septum at the scar border (red in the map), where the wavefront exits at the start of the VT beat and reenters at the end of the beat to complete the LV epicardial clockwise reentry pattern (white arrows). In this region, ECGI reconstructed low-amplitude, highly fractionated electrograms, consistent with electrical-scar substrate. Immediately before each VT beat, localized presystolic activity was observed at sites along the inferior scar border (see Online Movie I), indicating exit sites of activation fronts that propagated slowly through viable pathways in the scar substrate. The high curvature reentrant wavefront rotates around the scar (white arrows in Figure 5B; see Online Movie I).

It should be noted that determination of activation times in a region of scar is a challenging task. The time of local activation is determined from the electrogram as the instant of steepest negative deflection (so called “intrinsic deflection”). As shown above, electrograms within a scar substrate could be fractionated with multiple deflections, sometimes of similar magnitude and steepness. These deflections reflect activation of neighboring regions (“islands”) of surviving myocardium. The global activation sequence can be constructed by assigning a single (average) activation time. However, high resolution isochrones within the scar should consider each deflection distinctly. This requires careful interpretation and editing of the electrogram, considering not only its temporal properties, but also the spatial/temporal relationships to its neighbors.

Atrial Fibrillation (AF)

The substrate for atrial fibrillation is dynamic, with AF itself inducing remodeling and substrate changes that promote AF ("AF begets AF")[53]. Atrial remodeling is multi-factorial. It includes electrical remodeling of cellular electrophysiologic components (ion channels), resulting in shortening of the action potential and thus facilitating reentry[54]. Structural remodeling, in particular interstitial fibrosis, contributes to AF by providing a heterogeneous substrate that supports slow discontinuous conduction and development of conduction block, and can lead to breakup and fragmentation of propagating wavefronts[55]. Abnormal calcium cycling in remodeled atrial cells could underlie focal ectopic activity in AF[54]. As remodeling progresses, these multi-factorial changes interact to form a complex substrate for atrial excitation during AF.

In a recent study, ECGI activation maps of AF in 26 patients were analyzed in terms of complexity of patterns[56]. Within a diverse population of AF patients (including paroxysmal, persistent and longstanding persistent AF)[57], activation patterns were variable. The most common epicardial pattern during AF consisted of multiple wavelets together with activity from focal sites near the pulmonary veins. In general, complexity of the activation pattern (classified in terms of number of wavelets and focal sites) increased with longer clinical history of AF (i.e. with increased AF duration, implying longer, more progressed remodeling). Examples are provided in Figures 6 and 7; they serve to illustrate the effect of substrate remodeling progression on the complexity of the AF activation pattern, rather than provide insights into the basic mechanisms of AF. For discussion of mechanisms, the reader is referred to the original report on the ECGI AF study[56].

Figure 6 shows the activation pattern of paroxysmal nonsustained AF in a young patient with structurally normal heart. AF was induced during an EP study. The pattern is relatively simple; it is that of a single spiral wave (rotor), with a broad sweeping wavefront that involves both atria and rotates in a counter clockwise fashion. A similar example of paroxysmal AF is shown in Online Movie II. In comparison, the pattern of long-standing persistent AF in Figure 7 and Online Movie III is of much greater complexity. The movie shows 900 ms of continuous AF imaging. There are at least four co-existing wavelets, characterized by high degree of wavefront curvature and wave breaks. Focal sites are seen near pulmonary veins. The time-lapsed ECGI maps of Figure 7 are representative of similar complexity at other times during AF. Of course, the activation pattern is dynamically changing.

The observations above rely on the ability of ECGI to map the AF activation sequence continuously on both atria with sufficient resolution. This can be difficult to achieve in some cases, as the body surface signals generated by AF are typically of low amplitude and body surface potential distributions are smoothed-out by the torso volume conductor (see Figure 6). In the examples of Figures 6 and 7 (and for the other patients in the original AF study), a clear signal from atrial activation during AF was present in the body surface ECG (see lead II tracings). Several minutes of data were recorded from each patient. T-Q segments were used for analysis of AF. By considering at least 5 AF activation movies (ranging from 500 to 1000 ms) for each patient, non-physiological artifacts were minimized. Because ventricular signals are typically of much greater magnitude than the atrial signals, it might be necessary in some cases of AF with normal AV conduction to remove the ventricular signals by QRS(T) subtraction algorithms, or to apply AV blocking drugs to produce long continuous recordings of atrial signals of adequate quality.

Dispersion of Repolarization

Abnormal repolarization of the cardiac action potential can be the result of genetic mutations in ion channel proteins or other auxiliary proteins (e.g. the long QT syndrome[58]), disease processes (e.g. ischemia[59]), or the effects of various drugs. It can produce the two components that generate cardiac arrhythmias: the substrate and the trigger. A trigger associated with abnormal repolarization is early afterdepolarization (EAD). The substrate is steep regional repolarization gradients, or "dispersion of repolarization," that create spatial asymmetry of excitability and conditions for unidirectional block and reentry. Unlike the electrical substrate associated with a scar, where conduction properties are affected by pathological structural changes, steep dispersion of repolarization can exist in structurally normal myocardium. ECGI can image, noninvasively, not only the sequence of activation (examples in previous sections) but also the pattern of epicardial repolarization. The time of activation and the time of repolarization at a given location are determined from the ECGI - reconstructed electrogram. Activation time is determined as the time of maximum negative derivative on the QRS segment. Recovery time is the time of maximum derivative on the T-wave. Recovery times are determined by both the activation sequence and the local repolarization. Activation recovery interval (ARI) is the difference between recovery time and activation time; ARI reflects intrinsic repolarization properties, and is a surrogate for local action potential duration[60,61].

Early repolarization syndrome is defined in terms of its electrocardiographic signature, i.e. significant elevation of the QRS –ST segment junction in the inferior or lateral precordial leads[62,63,64]. It has long been considered to be benign[65]. However, it was recently shown to be more prevalent in patients with a history of idiopathic ventricular fibrillation (31.1% vs. 5% in control)[63,64]. Because of its non-specificity, the ECG signature does not provide a conclusive definition of the ventricular electrical substrate, as QRS prolongation and J-point elevation could reflect delayed activation and not necessarily early repolarization. ECGI was used to image the early repolarization substrate and to test the hypothesis that it involves accelerated repolarization rather than delayed activation; an example is provided in Figure 8[66].

Figure 8, top panel shows the ECGI activation map during sinus rhythm, with activation starting from the superior anterior septum (a variant of normal ventricular activation) followed by activation of the anterior RV and LV in an apex-to-base fashion. This activation sequence is normal and excitation spreads uniformly; there is no evidence for slow conduction or regions of abnormal delayed activation. Figure 8, middle panel depicts the ECGI repolarization ARI map for the same sinus beat. Strikingly, there are regions of very short ARI in mid-anterolateral RV (ARI =140 ms, dark blue, marked by 1 in RAO view) and inferior-basal RV (ARI =160 ms, light blue, marked by 3 in LPO view). These short ARIs reflect short action potentials in these regions. Corresponding ARI values in normal human ventricles are 235±21ms. Importantly for arrhythmogenesis, there are very steep repolarization gradients in these regions; 107.4 ms/cm in region 1 and 102.2 ms/cm in region 3. For comparison, ARI gradients in normal hearts range from 4.5 ms/cm to 11.3 ms/cm. ECGI-reconstructed electrograms from the regions of short ARI show marked elevation of the QRS-ST segment junction (inset 1), whereas those from neighboring regions do not show any evidence of early repolarization (inset 2).

During the ECGI procedure, the patient had several premature ventricular complexes (PVC) of identical morphologies. The bottom panel of Figure 8 shows ECGI-imaged epicardial potential maps for early activation (left) and repolarization (right) during a PVC. The local negative potential minimum of early activation (asterisk, dark blue) locates the PVC origin. Note that the PVCs originated from the apical region, remote to the area of steep dispersion

of repolarization. If the PVC excitation wave interacts with the substrate of steep dispersion in a specific way (at a particular velocity, direction, orientation and time window), unidirectional block can occur and reentrant arrhythmia induced. This, of course, is a probabilistic event that requires co-occurrence of multiple specific conditions.

In summary, ECGI of early repolarization identified normal ventricular activation during sinus rhythm, but abnormal repolarization with areas of very short ARIs (reflecting the short action potentials) as the substrate in this case. The resulting local dispersion of repolarization creates steep excitability gradients that provide the substrate for unidirectional block and reentry. The PVC excitation wave could provide the trigger for initiation of arrhythmic reentrant excitation in this substrate.

An ECGI study showed that repolarization abnormalities also occur in patients with the Wolff-Parkinson –White (WPW) syndrome[67]. In the preexcited rhythm, ARI was prolonged (349±6 ms) in the area of preexcitation leading to high base-to-apex ARI dispersion of 95±9 ms (normal is ~ 40 ms).The ARI dispersion remained the same 45 minutes after ablation of the accessory pathway, although the activation sequence was restored to normal. ARI dispersion was still high (79±9 ms) 1 week later and returned to normal (45±6 ms) 1 month after ablation. The 1-month time course is consistent with transcriptional reprogramming and remodeling of ion channels. It should be added that the ECGI determined preexcitation sites were consistent with sites of successful ablation in all cases. Accurate noninvasive determination of pre-excitation in WPW patients was also reported with the model-based activation time method[19].

Concluding Remarks

The topic of this review is the noninvasive imaging of electrophysiologic substrates using ECGI. The article is therefore limited to examples of substrate reconstructions and does not address the broader applications of ECGI in the study of arrhythmia mechanisms and in clinical practice. Being a noninvasive method, ECGI can serve both as a research tool for investigating the basic mechanisms of human cardiac arrhythmias, and as a clinical tool for diagnosis and guidance of therapy. We have published examples of both; the reader is referred to the research section of http://rudylab.wustl.edu for additional information and a list of references.

The examples of electrophysiologic substrate imaging in this article are representative of data from several studies. These data demonstrate the variability of substrate properties and characteristics between individual patients with similar diagnoses and pathologies. This is evident in the HF data of Figure 2, where native LV activation was heterogeneous among patients, with different spatial patterns of slow conduction and conduction block and different regions of latest activation. This variability has important clinical consequences, as optimal LV lead placement for CRT depends on the substrate properties. The choice of lead location should consider the sequence of activation (i.e., pacing from the region of most delayed activation to maximize synchrony) *and* the electrophysiologic properties of the substrate (avoiding electrode placement near extensive block regions and regions of slow conduction). This information could be obtained noninvasively with ECGI before CRT implantation, for guidance of electrode placement in a substrate-dependent individualized manner.

Similarly, the AF study highlights the coexistence of a variety of mechanisms and variable complexity among patients. ECGI can map the dynamically changing activation sequence of AF and may have a role in guidance of therapy. It could help to identify AF patients who are likely (or unlikely) to benefit from catheter or surgical ablation, depending on the

complexity of their atrial activation during AF. It could also help to plan a patient-specific ablation strategy, tailored to repetitive activation patterns in the individual patient's heart.

Variability also exists in the post-MI scar substrate. The substrate is characterized by heterogeneous scar with surviving myocardial fibers that support slow, discontinuous conduction. However, most patients with ischemic cardiomyopathy never develop VT. Efforts to quantify VT risk in this population have shown associations with scar burden and QRS fragmentation. A useful role for ECGI could be in noninvasive risk stratification for VT in ischemic cardiomyopathy patients. To this end, we compared ECGI from ischemic cardiomyopathy patients with or without history of VT. Preliminary results[68] show that patients with VT had a larger total electrical scar burden, greater electrogram fragmentation(reflecting greater heterogeneity of the substrate), and more late deflections ("late potentials") on the electrograms.

The noninvasive nature of ECGI makes it well suited for follow-up repeated studies over time. In the context of electrical substrate imaging, it could be used to assess the progression of substrate remodeling (e.g., degree of electrical heterogeneity of scar, steepness and extent of dispersion of repolarization) and the consequences of interventions such as ablation, reverse remodeling with CRT, or changes to the repolarization gradients due to drug therapy.

As explained in the Methods section, our approach to ECGI (reconstruction of epicardial potentials) limits solutions to the epicardial surface of the heart. This choice stems from several considerations: 1. The solution can be validated by comparison to directly recorded raw data (as in the tank-torso experiments and intra-operative mapping studies), without additional data processing (e.g., determination of activation times) that in itself could be a source of error. 2. Extension to the endocardium or intramural myocardium requires additional assumptions that may not be consistent with properties of excitation in a given patient's heart, thus biasing the results. 3. Epicardial potentials contain information on intramural and endocardial activation even before the epicardium is activated. As we have demonstrated[14], from the evolving pattern of epicardial potentials and electrogram morphology (presence or absence of r-wave) the intramural depth of an ectopic arrhythmic source can be estimated. Also, a study demonstrated how the intramural and septal sequence of reentrant activation during VT could be deduced from analysis of epicardial electrograms, potential maps and isochrones reconstructed with ECGI[69]. If needed, ECGI epicardial mapping and catheter endocardial mapping (in a limited region identified by ECGI) could be conducted simultaneously, providing data from both surfaces. 4. There is increasing evidence that many clinical VTs involve epicardial components or originate in the sub-epicardium. This realization led to the development of a method for transthoracic catheter ablation of epicardial sites[70]. 5. Importantly, ECGI in terms of potentials reconstructs the entire time course of electrograms during the cardiac cycle and generates potential maps, activation isochrones and repolarization patterns. Activation time mapping constructs only one time point on the electrogram (the steepest negative deflection point on the QRS); it does not consider all other information that electrograms contain, including repolarization. In the context of electrical substrate imaging with ECGI, reconstructing entire electrograms is of particular importance. As shown by the examples of this review, post-MI scar substrate is reflected in the electrogram magnitude, multiple deflections along its entire time course, and presence of delayed deflections ("late potentials"). Also, imaging the substrate of steep repolarization gradients requires reconstruction of repolarization and ARIs, not only activation.

Supplementary Material

Refer to Web version on PubMed Central for supplementary material.

Acknowledgments

Many thanks to Tally Portnoi for her help in preparing the manuscript and to Junjie Zhang for his help with figures and movies. Yoram Rudy is the Fred Saigh Distinguished Professor at Washington University in St. Louis.

Sources of Funding

Studies presented in this article were supported by grants R01-HL33343 and R01-HL49054 from the NIH-National Heart, Lung and Blood Institute (to Y. Rudy)

Non-standard Abbreviations and Acronyms

(ECGI)	Electrocardiographic imaging
(MI)	Myocardial infarction
(EP)	Electrophysiology
(AF)	Atrial fibrillation
(GMRes)	Generalized minimal residual
(CT)	Computed tomography
(CRT)	Cardiac Resynchronization Therapy
(HF)	Heart failure
(LBBB)	Left bundle branch block
(LV)	Left ventricle
(RV)	Right ventricle
(LAD)	Left anterior descending coronary artery
(VT)	Ventricular Tachycardia
(SPECT)	Single-photon emission computed tomography
(EAD)	Early afterdepolarization
(ARI)	Activation recovery interval
(PVC)	Premature ventricular complex
(EGM)	Epicardial electrogram
(ESM)	Electrical scar map
(LAO)	Left anterior oblique
(RAO)	Right anterior oblique
(LSPV)	Left superior pulmonary vein
(LIPV)	Left inferior pulmonary vein
(RSPV)	Right superior pulmonary vein
(RIPV)	Right inferior pulmonary vein
(RA)	Right atrium

(RAA)	Right atrial appendage
(LAA)	Left atrial appendage
(TV)	Tricuspid valve
(MV)	Mitral valve
(LA)	Left atrium
(AO)	Aorta

References

1. Rudy, Y. Mathematical modeling of complex biological systems: from genes and molecules to organs and organisms: heart. Simulation and Modeling. In: Weinstein, H.; Egelman, EH., editors. Comprehensive Biophysics. Vol. 9. Academic Press; Oxford: 2012. p. 268-327.
2. Ursell PC, Gardner PI, Albana A, Fenoglio JJ Jr, Wit AL. Structural and electrophysiological changes in epicardial border zone of canine myocardial infarcts during healing. Circ Res. 1985; 56:436–451. [PubMed: 3971515]
3. Wit AL, Janse MJ. Experimental models of ventricular tachycardia and fibrillation caused by ischemia and infarction. Circulation. 1992; 85:132–42.
4. Ramanathan C, Ghanem RN, Jia P, Ryu K, Rudy Y. Noninvasive electrocardiographic imaging for cardiac electrophysiology and arrhythmia. Nat Med. 2004; 10:422–428. [PubMed: 15034569]
5. Ramanathan C, Jia P, Ghanem RN, Ryu K, Rudy Y. Activation and repolarization of the normal human heart under complete physiological conditions. Proc Natl Acad Sci U S A. 2006; 103:6309–14. [PubMed: 16606830]
6. Plonsey, R.; Barr, RC. Bioelectricity—a quantitative approach. 3rd ed. Springer; New York: 2007.
7. Barr RC, Ramsey M III, Spach MS. Relating epicardial to body surface potential distributions by means of transfer coefficients based on geometry measurements. IEEE Trans Biomed Eng. 1977; 24:1–11. [PubMed: 832882]
8. Tikhonov, AN.; Arsenin, VY. Solution of Ill-Posed Problems. John Wiley and Sons; New York: 1977.
9. Colli Franzone P, Guerri L, Taccardi B, Viganotti C. The direct and inverse potential problems in electrocardiology: Numerical aspects of some regularization methods and application to data collected in isolated dog heart experiments. Lab Anal Numerica CNR. 1979:222.
10. Saad Y, Shultz MH. GMRes: a generalized minimal residual algorithm for solving nonsymmetric linear systems. SIAM J Sci Stat Comput. 1986; 7:856–869.
11. Ramanathan C, Jia P, Ghanem RN, Calvetti D, Rudy Y. Noninvasive Electrocardiographic Imaging (ECGI): application of the generalized minimal residual (GMRes) method. Ann Biomed Eng. 2003; 31:981–994. [PubMed: 12918913]
12. Rudy, Y.; Ramanathan, C.; Ghosh, S.; Zipes, DP. Noninvasive Electrocardiographic Imaging (ECGI): methodology and excitation of the normal human heart. In: Jalife, J., editor. Cardiac Electrophysiology: From Cell to Bedside. 5th ed. WB Saunders; Philadelphia: 2009. p. 467-472.
13. Oster HS, Taccardi B, Lux RL, Ershler PR, Rudy Y. Noninvasive Electrocardiographic Imaging: reconstruction of epicardial potentials, electrograms and isochrones, and localization of single and multiple electrocardiac events. Circulation. 1997; 96:1012–1024. [PubMed: 9264513]
14. Oster HS, Taccardi B, Lux RL, Ershler PR, Rudy Y. Electrocardiographic imaging: noninvasive characterization of intramural myocardial activation from inverse reconstructed epicardial potentials and electrograms. Circulation. 1998; 97:1496–1507. [PubMed: 9576431]
15. Burnes JE, Taccardi B, Rudy Y. A noninvasive imaging modality for cardiac arrhythmias. Circulation. 2000; 102:2152–2158. [PubMed: 11044435]
16. Burnes JE, Taccardi B, MacLeod RS, Rudy Y. Noninvasive Electrocardiographic Imaging of electrophysiologically abnormal substrate in infarcted hearts: a model study. Circulation. 2000; 101:533–540. [PubMed: 10662751]

17. Ghanem RN, Jia P, Ramanathan C, Ryu K, Markowitz A, Rudy Y. Noninvasive Electrocardiographic Imaging (ECGI): comparison to intraoperative mapping in patients. Heart Rhythm. 2005; 2:339–354. [PubMed: 15851333]
18. Ghanem RN, Burnes JE, Waldo AL, Rudy Y. Imaging Dispersion of Myocardial Repolarization II. Noninvasive Reconstruction of Epicardial Measures. Circulation. 2001; 104:1306–1312. [PubMed: 11551884]
19. Berger T, Fischer G, Pfeifer B, Modre R, Hanser F, Trieb T, Roithinger FX, Stuehlinger M, Pachinger O, Tilg B, Hintringer F. Single-Beat Noninvasive Imaging of Cardiac Electrophysiology of Ventricular Pre-Excitation. J Amer College Cardiol (JACC). 2006; 48:2045–52.
20. Berger T, Pfeifer B, Hanser FF, Hintringer F, Fischer G, et al. Single-Beat Noninvasive Imaging of Ventricular Endocardial and Epicardial Activationin Patients Undergoing CRT. PLoS ONE. 2011; 6(1):e16255. doi:10.1371/journal.pone.0016255. [PubMed: 21298045]
21. Lloyd-Jones D, Adams RJ, Brown TM, Carnethon M, Dai S, de Simone G, Ferguson TB, Ford E, Furie K, Gillespie C, Go A, Greenlund K, Haase N, Hailpern S, Ho PM, Howard V, Kissela B, Kittner S, Lackland D, Lisabeth L, Marelli A, McDermott MM, Meigs J, Mozaffarian D, Mussolino M, Nichol G, Roger VL, Rosamond W, Sacco R, Sorlie P, Roger VL, Stafford R, Thom T, Smoller S, Wong ND, Wylie-Rosett J. Heart disease and stroke statistics—2010 update: a report from the American Heart Association. Circulation. 2010; 121:e46–e215. [PubMed: 20019324]
22. Zipes DP, Camm AJ, Borggrefe M, Buxton AE, Chaitman B, Fromer M, Gregoratos G, Klein G, Moss AJ, Myerburg RJ, Priori SG, Quinones MA, Roden DM, Silka MJ, Tracy C. ACC/AHA/ESC 2006 Guidelines for Management of Patients With Ventricular Arrhythmias and the Prevention of Sudden Cardiac Death: A Report of the American College of Cardiology/American Heart Association Task Force and the European Society of Cardiology Committee for Practice Guidelines (Writing Committee to Develop Guidelines for Management of Patients With Ventricular Arrhythmias and the Prevention of Sudden Cardiac Death): Developed in Collaboration With the European Heart Rhythm Association and the Heart Rhythm Society. Circulation. 2006; 114:e385–e484. [PubMed: 16935995]
23. Tomaselli GF, Marban E. Electrophysiological remodeling in hypertrophy and heart failure. Cardiovasc Res. 1999; 42:270–283. [PubMed: 10533566]
24. Janse MJ. Electrophysiological changes in heart failure and their relationship to arrhythmogenesis. Cardiovasc Res. 2004; 61:208–17. [PubMed: 14736537]
25. Pu J, Boyden PA. Alterations of Na^+ currents in myocytes from epicardial border zone of the infarcted heart: a possible ionic mechanism for reduced excitability and postrepolarization refractoriness. Circ Res. 1997; 81:110–9. [PubMed: 9201034]
26. Akar FG, Spragg DD, Tunin RS, Kass DA, Tomaselli GF. Mechanisms underlying conduction slowing and arrhythmogenesis in nonischemic dilated cardiomyopathy. Circ Res. 2004; 95:717–25. [PubMed: 15345654]
27. Maguy A, Le Bouter S, Comtois P, Chartier D, Villeneuve L, Wakili R, Nishida K, Nattel S. **Ion** Channel Subunit Expression Changes in Cardiac Purkinje Fibers A Potential Role in Conduction Abnormalities Associated With Congestive Heart Failure. Circ Res. 2009; 104:1113–1122. [PubMed: 19359601]
28. Pogwizd SM, Bers DM. Cellular basis of triggered arrhythmias in heart failure. Trends Cardiovasc Med. 2004; 14:61–6. [PubMed: 15030791]
29. Raman, S.; Donnally, M. Cardiac magnetic resonance assessment of ventricular dyssynchrony. In: Abraham, WT.; Baliga, RR., editors. Cardiac Resynchronization Therapy in Heart Failure. Lippincott Williams & Wilkins; Philadelphia: 2010. p. 76-80.
30. Dimaano, VLJ.; Abraham, TP. The role of echocardiography and tissue doppler imaging in optimal cardiac resynchronization therapy. In: Abraham, WT.; Baliga, RR., editors. Cardiac Resynchronization Therapy in Heart Failure. Lippincott Williams & Wilkins; Philadelphia: 2010. p. 59-75.
31. Auricchio A, Fantoni C, Regoli F, Carbucicchio C, Goette A, Geller C, Kloss M, Klein H. Characterization of left ventricular activation in patients with heart failure and left bundle-branch block. Circulation. 2004; 109:1133–1139. [PubMed: 14993135]

32. Jia P, Ramanathan C, Ghanem RN, Ryu K, Varma N, Rudy Y. Electrocardiographic imaging of cardiac resynchronization therapy in heart failure: observations of variable electrophysiologic responses. Heart Rhythm. 2006; 3:296–310. [PubMed: 16500302]
33. Fung JW, Yu CM, Yip G, Zhang Y, Chan H, Kum CC, Sanderson JE. Variable left ventricular activation patterns in patients with heart failure and left bundle branch block. Heart (Br Card Soc). 2004; 90:17–19.
34. Bradley DJ, Bradley EA, Baughman KL, Berger RD, Calkins H, Goodman SN, Kass DA, Powe NR. Cardiac resynchronization and death from progressive heart failure: a meta-analysis of randomized controlled trials. JAMA. 2003; 289:730–40. [PubMed: 12585952]
35. Aiba T, Hesketh GG, Barth AS, Liu T, Daya S, Chakir K, Dimaano VL, Abraham TP, O'Rourke B, Akar FG, Kass DA, Tomaselli GF. Electrophysiological consequences of dyssynchronous heart failure and its restoration by resynchronization therapy. Circulation. 2009; 119:1220–30. [PubMed: 19237662]
36. Silva JN, Ghosh S, Bowman TM, Rhee EK, Woodard PM, Rudy Y. Cardiac Resynchronization Therapy in Pediatric Congenital heart Disease: Insights from Noninvasive Electrocardiographic Imaging. Heart Rhythm. 2009; 6:1178–1185. [PubMed: 19632630]
37. Liang Y, Pan W, Su Y, Ge J. Meta-Analysis of Randomized Controlled Trials Comparing Isolated Left Ventricular and Biventricular Pacing in Patients With Chronic Heart Failure. Am J Cardiol. 2011; 108:1160–1165. [PubMed: 21813108]
38. Thibault B, Ducharme A, Harel F, et al. Left ventricular versus simultaneous biventricular pacing in patients with heart failure and a QRS complex ≥120 milliseconds. Circulation. 2011; 124:2874–2881. [PubMed: 22104549]
39. van Gelder BM, Bracke FA, Meijer A, Pijls NH. The hemodynamic effect of intrinsic conduction during left ventricular pacing as compared to biventricular pacing. J Am Coll Cardiol. 2005; 46:2305–2310. [PubMed: 16360063]
40. Martin DO, Lemke B, Birnie D, Krum H, Lee KF, Aonuma K, Gasparini M, Starling RC, Milasinovic G, Rogers T, Sambelashvili A, Houmsse M, John Gorcsan J III. Investigation of a novel algorithm for synchronized leftventricular pacing and ambulatory optimization of cardiacresynchronization therapy: Results of the adaptive CRT trial. Heart Rhythm. 2012; xx:xxx. published ahead of print.
41. Janse MJ, Wit AL. Electrophysiological mechanisms of ventricular arrhythmias resulting from myocardial ischemia and infarction. Physiol Rev. 1989; 69:1049–1169. [PubMed: 2678165]
42. Rutherford SL, Trew ML, Sands GB, LeGrice IJ, Smaill BH. High-resolution 3-dimensional reconstruction of the infarct border zone: impact of structural remodeling on electrical activation. Circ Res. 2012; 111:301–311. [PubMed: 22715470]
43. Pinto JM, Boyden PA. Electrical remodeling in ischemia and infarction. Cardiovasc Res. 1999; 42:284–297. [PubMed: 10533567]
44. de Bakker JM, Stein M, van Rijen HV. Three-dimensional anatomic structure as substrate for ventricular tachycardia/ventricular fibrillation. Heart Rhythm. 2005; 2:777–9. [PubMed: 15992738]
45. Gardner PI, Ursell PC, Fenoglio JJ Jr, Wit AL. Electrophysiologic and anatomic basis for fractionated electrograms recorded from healed myocardial infarcts. Circulation. 1985; 72:596–611. [PubMed: 4017211]
46. Klein H, Karp RB, Kouchoukos NT, Zorn GL Jr, James TN, Waldo AL. Intraoperative electrophysiologic mapping of the ventricles during sinus rhythm in patients with a previous myocardial infarction: Identification of the electrophysiologic substrate of ventricular arrhythmias. Circulation. 1982; 66:847–53. [PubMed: 7116600]
47. Josephson ME, Wit AL. Fractionated electrical activity and continuous electrical activity: fact or artifact? Circulation. 1984; 70:529–32. [PubMed: 6478558]
48. Kleber AG, Rudy Y. Basic mechanisms of cardiac impulse propagation and reentrant arrhythmias. Physiol Rev. 2004; 84:431–488. [PubMed: 15044680]
49. Simson MB, Untereker WJ, Spielman SR, Horowitz LN, Marcus NH, Falcone RA, Harken AH, Josephson ME. Relation between late potentials on the body surface and directly recorded

fragmented electrograms in patients with ventricular tachycardia. Am J Cardiol. 1983; 51:105–12. [PubMed: 6849248]

50. Wilber, DJ. Substrate-based ablation of postinfarction ventricular tachycardia. In: Wilber, DJ.; Packer, DL.; Stevenson, WG., editors. Catheter Ablation of Cardiac Arrhythmias; Basic Concepts and Clincial Applications. 3rd ed.. Blackwell Futura; Malden, MA: 2008. p. 326-339.
51. Cuculich PS, Zhang J, Wang Y, Desouza KA, Vijayakumar R, Woodard PK, Rudy Y. The electrophysiologic cardiac ventricular substrate in patients after myocardial infarction: noninvasive characterization with electrocardiographic imaging. J Am Coll Cardiol. 2011; 58:1893–1902. [PubMed: 22018301]
52. Wang Y, Cuculich PS, Zhang J, Desouza KA, Vijayakumar R, Chen J, Faddis MN, Lindsay BD, Smith TW, Rudy Y. Noninvasive Electroanatomic Mapping of Human Ventricular Arrhythmias with Electrocardiographic Imaging. Sci Transl Med. 2011; 3:191–200.
53. Wijffels MC, Kirchhof CJ, Dorland R, Allessie MA. Atrial fibrillation begets atrial fibrillation: a study in awake chronically instrumented goats. Circulation. 1995; 92:1954–1968. [PubMed: 7671380]
54. Nattel S, Burnstein B, Dorbev D. Atrial remodeling and atrial fibrillation: mechanisms and implications. Circ Arrhythm Electrophysiol. 2008; 1:62–73. [PubMed: 19808395]
55. Burstein B, Nattel S. Atrial fibrosis: mechanisms and clinical relevance in atrial fibrillation. J Am Coll Cardiol. 2008; 51:802–809. [PubMed: 18294563]
56. Cuculich PS, Wang Y, Lindsay BD, Faddis MN, Schuessler RB, Damiano RD, Li L, Rudy Y. Noninvasive characterization of epicardial activation in humans with diverse atrial fibrillation patterns. Circulation. 2010; 122:1364–1372. [PubMed: 20855661]
57. Oral, H. Atrial Fibrillation: Mechanisms, Features, and Management. In: Zipes, DP.; Jalife, J., editors. Cardiac Electrophysiology: From Cell to Bedside. 5th ed.. WB Saunders; Philadelphia: 2009. p. 577-588.
58. Schwartz PJ, Stramba-Badiale M, Crotti L, Pedrazzini M, Besana A, Bosi G, Gabbarini F, Goulene K, Insolia R, Mannarino S, Mosca F, Nespoli A, Rimini A, Rosati E, Salice P, Spazzolini C. Prevalence of the congenital Long-QT syndrome. Circulation. 2009; 120:1761–1767. [PubMed: 19841298]
59. Shaw RM, Rudy Y. Electrophysiologic Effects of Acute Myocardial Ischemia: A Theoretical Study of Altered Cell Excitability and Action Potential Duration. Cardiovasc Res. 1997; 35:256–272. [PubMed: 9349389]
60. Haws CW, Lux RL. Correlation between in vivo transmembrane action potential durations and activation-recovery intervals from electrograms: effects of interventions that alter repolarization time. Circulation. 1990; 81:281–8. [PubMed: 2297832]
61. Coronel R, de Bakker JM, Wilms-Schopman FJG, Opthof T, Linnenbank AC, Belterman CN, Janse MJ. Monophasic action potentials and activation recovery intervals as measures of ventricular action potential duration: experimental evidence to resolve some controversies. Heart Rhythm. 2006; 3:1045–1050.
62. Mehta M, Jain AC, Mehta A. Early repolarization. Clin Cardiol. 1999; 22:59–65. [PubMed: 10068841]
63. Haïssaguerre M, Derval N, Sacher F, Jesel L, Deisenhofer I, de Roy L, Pasquié JL, Nogami A, Babuty D, Yli-Mayry S, De Chillou C, Scanu P, Mabo P, Matsuo S, Probst V, Le Scouarnec S, Defaye P, Schlaepfer J, Rostock T, Lacroix D, Lamaison D, Lavergne T, Aizawa Y, Englund A, Anselme F, O'Neill M, Hocini M, Lim KT, Knecht S, Veenhuyzen GD, Bordachar P, Chauvin M, Jais P, Coureau G, Chene G, Klein GJ, Clémenty J. Sudden cardiac arrest associated with early repolarization. New Engl J Med. 2008; 358:2016–23. [PubMed: 18463377]
64. Miyazaki S, Shah AJ, Haissaguerre M. Early repolarization syndrome—a new electrical disorder associated with sudden cardiac death. Circ J. 2010; 74:2039–44. [PubMed: 20838009]
65. Boineau JP. The early repolarization variant—normal or a marker of heart disease in certain subjects. J Electrocardiol. 2007; 401(3):e11–6. [PubMed: 17081556]
66. Ghosh S, Cooper DH, Vijayakumar R, Zhang J, Pollak S, Haissaguerre M, Rudy Y. Early repolarization associated with sudden death: insights from noninvasive Electrocardiographic Imaging (ECGI). Heart Rhythm. 2010; 7:534–537. [PubMed: 20153422]

67. Ghosh S, Rhee EK, Avari JN, Woodard PK, Rudy Y. Cardiac Memory in WPW Patients: Noninvasive Imaging of Activation and Repolarization before and after Catheter Ablation. Circulation. 2008; 118:907–915. [PubMed: 18697818]

68. Zhang J, Cooper DH, Desouza KA, Marrus SB, Fansler DR, Cuculich PS, Smith TW, Rudy Y. ECG Imaging (ECGI) of Electrophysiologic Substrate in Ischemic Cardiomyopathy: Differences in Patients With and Without Ventricular Tachycardia (VT). Heart Rhythm. 2011; 8(5S):S480.

69. Burnes JE, Taccardi B, Ershler PP, Rudy Y. Noninvasive ECG Imaging of Substrate and Intramural Ventricular Tachycardia in Infarcted Hearts. J Amer College Cardiol (JACC). 2001; 38:2071–2078.

70. Sosa E, Scanavacca M, D'Avila A, Piccioni J, Sanchez O, Velarde JL, Silva M, Reolao B. Endocardial and epicardial ablation guided by nonsurgical transthoracic epicardial mapping to treat recurrent ventricular tachycardia. J Cardiovasc Electrophysiol. 1998; 9:229–239. [PubMed: 9580377]

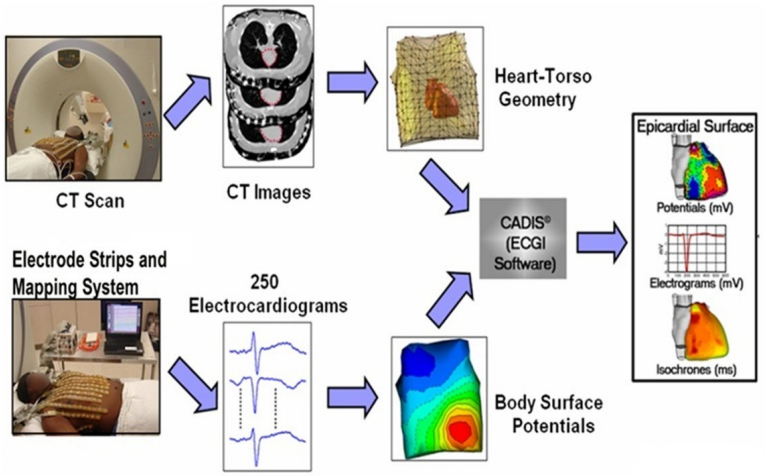

Figure 1.

The ECGI procedure. Bottom: The electrical data. 250 electrocardiograms over the entire torso surface are recorded simultaneously to generate body surface potential maps every millisecond. Top: The geometrical data. CT scan provides the epicardial geometry and body-surface electrode positions in the same image. The electrical and geometrical data are combined and processed by the ECGI algorithms to reconstruct potentials, electrograms, activation isochrones and repolarization patterns on the surface of the heart. (Adapted from reference 4).

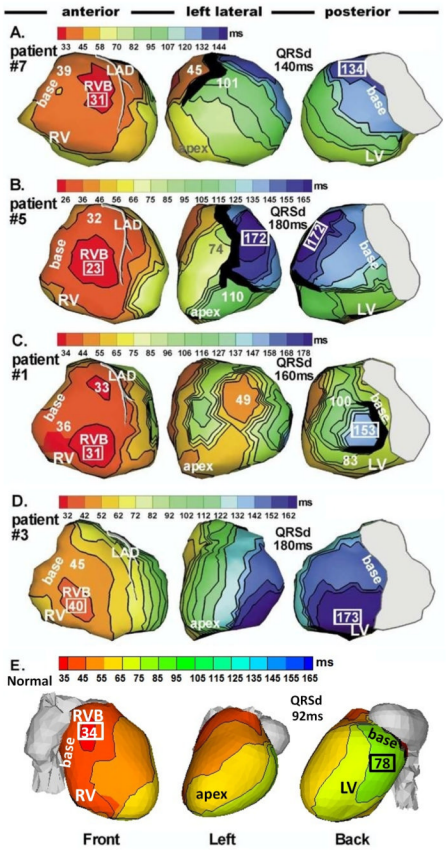

Figure 2.

Epicardial isochrone maps of native rhythm in four representative HF patients (A to D) and in a normal heart (E). Three views are shown for each heart, as indicated at the bottom. Thick black markings indicate conduction block. All HF maps show sequential activation of right ventricle (RV) followed by greatly delayed left ventricular (LV) activation (left bundle branch block, LBBB pattern). RV activation is similar in all patients and has a normal pattern with clearly identified anterior epicardial breakthrough (RVB) location. Details of LV activation vary among patients: A. Apical to lateral-basal conduction. B. Inferior to anterolateral conduction. C. Combined activation from apical, inferior and superior LV. D. Anterior to inferoposterior conduction. Note the variation of region of latest LV activation among the four HF hearts. E. Normal sinus rhythm. Note high degree of ventricular synchrony and absence of conduction delays or block. Numbers indicate activation times (from QRS onset) in milliseconds. QRSd = QRS duration (Adapted from reference 32, with permission).

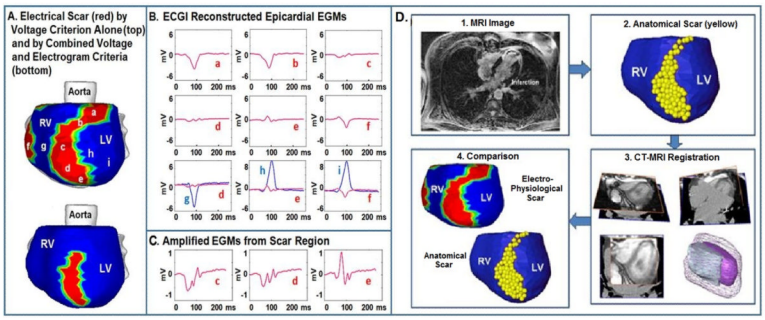

Figure 3.

Images of post-MI electrical and anatomical scar. A. Electrical scar is shown in red (left anterior oblique view). Top image is based on low voltage electrograms only. Bottom image includes the electrograms fractionation criterion. B. Representative electrograms from the scar (a-f, red) and outside the scar (g, h, i; blue). All scar electrograms are of low magnitude; electrograms c, d, and e are also fractionated, as can be easily appreciated from the expanded scale of panel C. Bottom row of panel B shows scar (red) and non-scar (blue) electrograms on the same scale to demonstrate the magnitude difference. D. Low voltage electrical scar (red) is compared to MRI-imaged anatomical scar (yellow). EGM = epicardial electrogram. From reference 51 with permission.

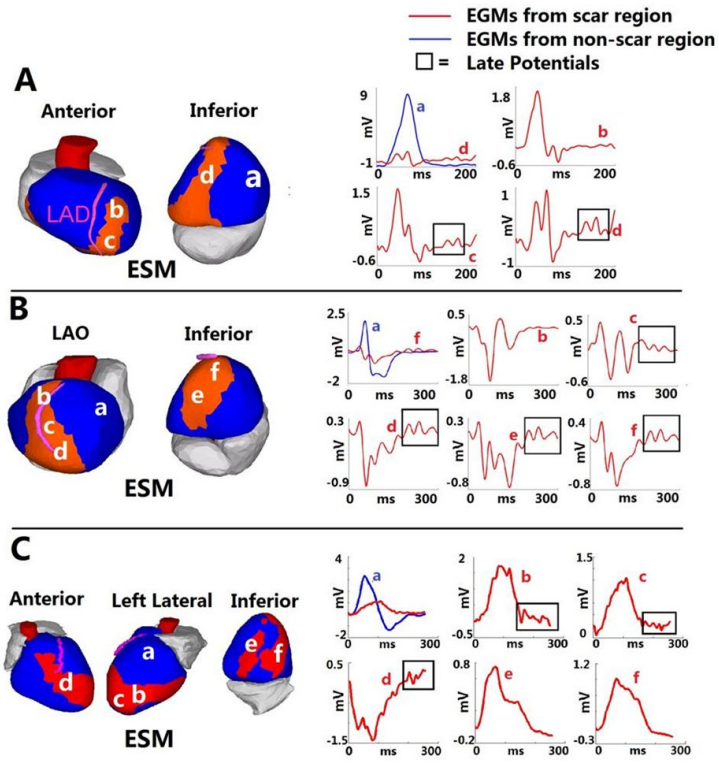

Figure 4.

Late potentials in a post-MI scar. Three examples are shown: A. Inferoseptal scar. B. Anteroapical scar. C. Complex anterior, apical and inferior infarction. Scar maps are presented on the left and selected electrograms on the right. Electrogram locations are indicated with letters. Late potentials (delayed deflections on the electrogram) are highlighted by frame. ESM = electrical scar map. LAO = left anterior oblique. From reference 51 with permission.

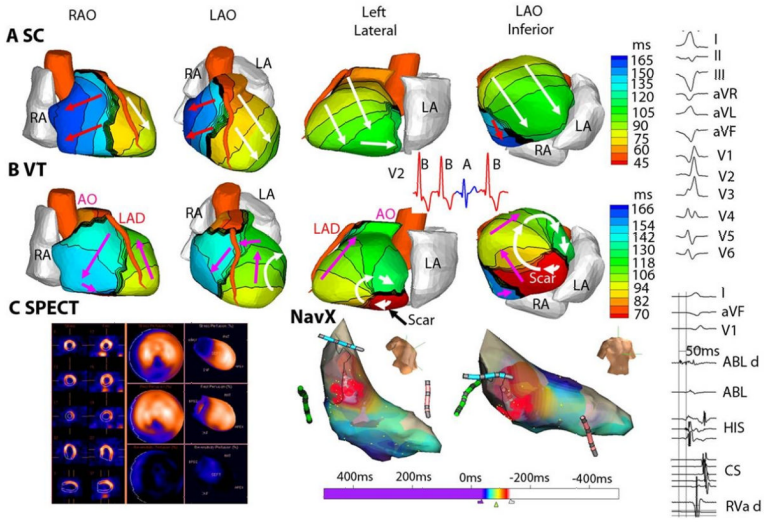

Figure 5.

Scar-related reentrant VT. The scar is inferobasal. A. Epicardial activation isochrones for a sinus capture (SC) beat. B. The activation pattern during VT beat. A clockwise reentry loop (white arrows in left lateral and LAO inferior views) is anchored to the scar. Pink arrows depict a wavefront propagating in a clockwise fashion into the RV. ECG lead V2 (inset) shows two VT beats (red, B) interrupted by a SC beat (blue, A) followed by another VT beat (VT is monomorphic). Online Movie I shows this entire sequence as imaged by ECGI. C. (left) single-photon emission computed tomography (SPECT) of inferobasal scar (blue). (Right) Endocardial activation during VT mapped with a NavX catheter (red is early; blue is late). Right column presents (top): Twelve lead body-surface ECG of VT; (bottom): signals recorded by the ablation catheter. LAO = left anterior oblique. RAO = right anterior oblique. See Online Movie I. From reference 52 with permission.

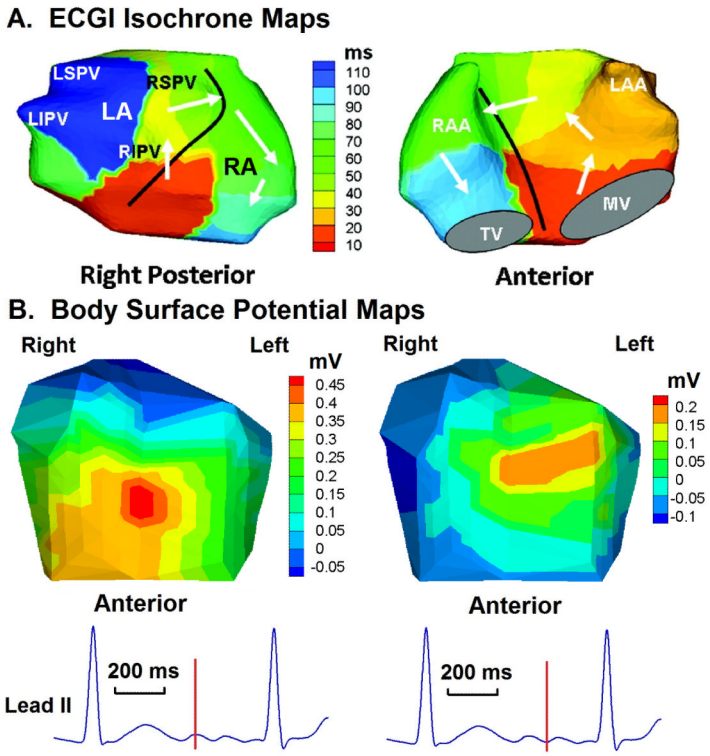

Figure 6.

Paroxysmal atrial fibrillation. A. A single bi-atrial spiral wave (rotor) drives the arrhythmia (white arrows). 100 ms of AF are depicted in the map (right posterior and anterior views). Black line marks the inter-atrial septum. B. Body surface potential maps at the two instances during AF marked on the ECG lead II at the bottom. Note the low voltages and simple (single-maximum) potential distribution, a consequence of the smoothing effect of the torso volume conductor. LSPV = left superior pulmonary vein. LIPV = left inferior pulmonary vein. RSPV = right superior pulmonary vein. RIPV = right inferior pulmonary vein. RA = right atrium. RAA = right atrial appendage. LA = left atrium. LAA = left atrial appendage. TV = tricuspid valve. MV = mitral valve. Online Movie II shows this repetitive pattern. Adapted from reference 56 with permission.

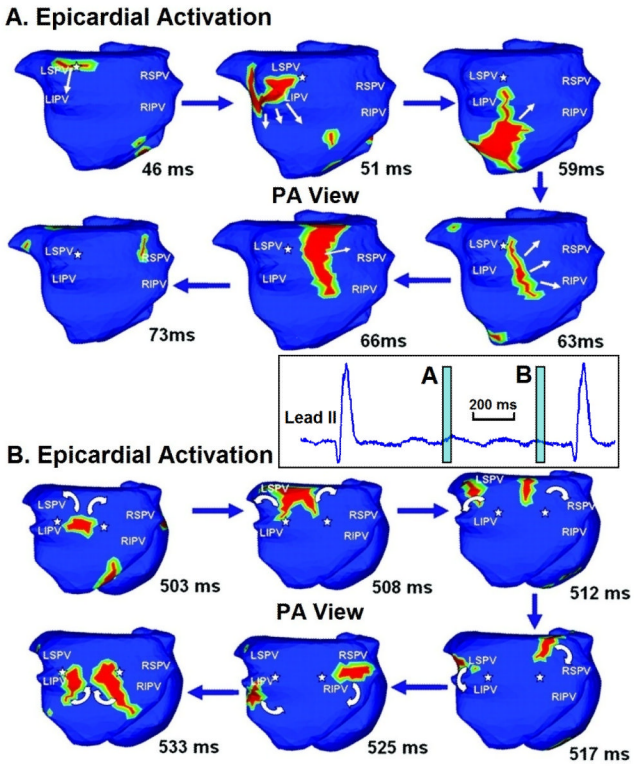

Figure 7.

Long-standing persistent atrial fibrillation. Time-lapse presentation of activation wavelets (red) during AF, shown in posterior-anterior (PA) view. (A) 46-73 ms. (B) 503-533 ms. White arrows indicate direction of wavelet propagation. White asterisks mark pivot points for wavelet rotation. The lead II inset between the panels shows the time windows (light blue) covered by the time-lapse frames in panels A and B. See Online Movie III. Adapted from reference 56 with permission.

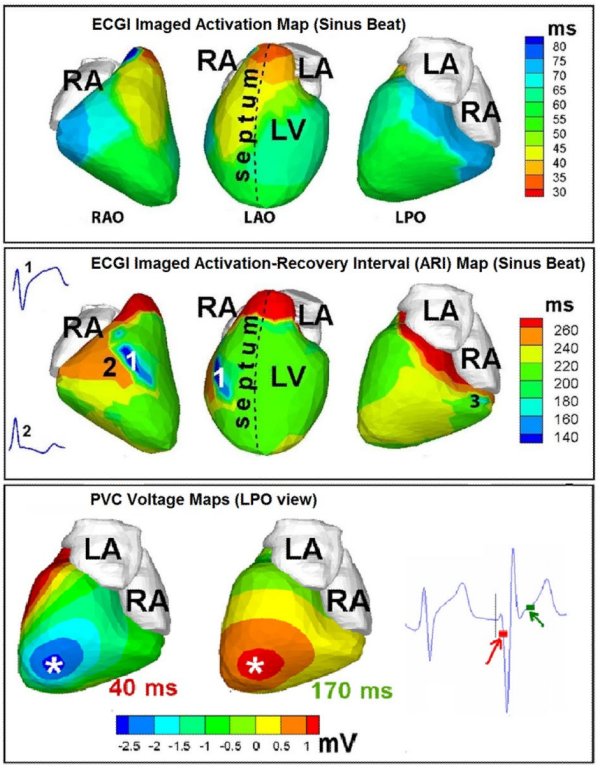

Figure 8.

Abnormal repolarization substrate in early repolarization syndrome. Top row: Activation isochrone maps during a sinus beat shown in three views (from left to right: right anterior oblique, left anterior oblique, left posterior oblique). Middle row: Repolarization ARI maps for the same sinus beat. Insets show two representative electrograms: (1) from the dark blue area with unusually short ARI, and (2) from an adjacent area. Bottom row: ECGI epicardial potential maps during early activation (40 ms, left) and at the start of repolarization (170 ms, right) of a PVC beat. The time points of the potential maps are shown on an ECG trace to the right of the maps. PVC = premature ventricular complex. Adapted from reference 66 with permission.